



ELSEVIER

Contents lists available at SciVerse ScienceDirect

Earth and Planetary Science Letters

journal homepage: www.elsevier.com/locate/epsl

Reconstruction of cave air temperature based on surface atmosphere temperature and vegetation changes: Implications for speleothem palaeoclimate records



David Domínguez-Villar^{a,b,*}, Ian J. Fairchild^b, Andy Baker^c, Rosa M. Carrasco^d, Javier Pedraza^e

^a Centro Nacional de Investigación sobre la Evolución Humana, Paseo Sierra de Atapuerca s/n, 09002 Burgos, Spain

^b School of Geography, Earth and Environmental Sciences, University of Birmingham, Edgbaston, B15 2TT Birmingham, United Kingdom

^c Connected Waters Initiative Research Centre, University of New South Wales, 110 King St. Manly Vale, 2093 NSW, Australia

^d Departamento de Ingeniería Geológica y Minera, Universidad de Castilla-La Mancha, Av. Carlos III s/n, 45071 Toledo, Spain

^e Departamento de Geodinámica, Universidad Complutense de Madrid, C/José Antonio Novais 12, 28040 Madrid, Spain

ARTICLE INFO

Article history:

Received 4 June 2012

Received in revised form

20 January 2013

Accepted 16 March 2013

Editor: G. Henderson

Available online 16 April 2013

Keywords:

temperature

thermal conduction

cave

palaeoclimate

speleothems

ABSTRACT

Cave temperature is a parameter of major importance for palaeoclimate studies based on speleothems since most proxies used are temperature-dependent. The general assumption that cave temperature reflects the mean annual surface atmosphere temperature (SAT) over the cave is based on a limited number of specific studies, and detailed mechanisms supporting this link are not properly described. Eagle Cave, in Spain, was used to understand the detailed mechanisms connecting SAT and cave temperature. A monitoring programme conducted from 2009 to 2011 allows the characterization of the thermal dynamics in the cave air. In the studied karstic environment thermal conduction is the main mechanism responsible for transferring the ground temperature signal to the cave. The calculated thermal diffusion coefficient is $0.756 \times 10^{-6} \pm 0.013 \text{ m}^2 \text{ s}^{-1}$. The SAT signal is recorded at the cave with a delay ranging from ~3 to 11 yr, depending on the thickness of the bedrock over the ceiling (5–18 m). A cave cooling of 2 °C has been recorded since mid-1970s, when cave temperature measurements were made. The application of a model exclusively based on thermal conduction of SAT does not reproduce the observed thermal changes. However, vegetation cover over the cave was modified dramatically during recent decades. This impacts ground temperature due to the changes in exposure to insolation and the modification of soil properties, which is eventually recorded in the cave. The incorporation of changes in vegetation cover in the model provides a realistic thermal reconstruction. The impact of vegetation cover was much more significant than SAT in order to explain the large thermal change in the cave over past decades. Thus, the cooling in Eagle Cave during past decades is mainly controlled by a variable decoupling from mean annual SAT as a result of the afforestation over the cave. The effect of this thermal decoupling on speleothem $\delta^{18}\text{O}$ records is potentially significant and should be considered when performing accurate palaeoclimate reconstructions.

© 2013 Elsevier B.V. All rights reserved.

1. Introduction

It is well known that many caves have a relatively stable temperature during the year in their sections away from the entrance (Moore, 1964). This cave air temperature has been related to the mean annual surface atmosphere temperature (SAT) at the exterior over the cave (Moore and Nicholas, 1964; Wigley and Brown, 1976; Moore and Sullivan, 1978). The implications of this

link are of major importance for palaeoclimate studies on cave records since their archives have the potential to record low-frequency changes in SAT. Many proxies recorded in speleothems are dependent on cave temperature. This is the case for oxygen stable isotopes (Epstein et al., 1953), some trace elements (Huang and Fairchild, 2001; Fairchild and Treble, 2009), the growth rate (Dreybrodt, 1981; Baker et al., 1998), or some biomarkers, as the glycerol dialkyl glycerol tetraethers (Schouten et al., 2007). Thus, some speleothem records have been interpreted as affected by changes in cave temperature, and hence reflecting long term variations in SAT (e.g., Dorale et al., 1992; Lauritzen and Lundberg, 1999). The assumption of a connexion between SAT and cave

* Corresponding author at: Centro Nacional de Investigación sobre la Evolución Humana, Paseo Sierra de Atapuerca s/n, 09002 Burgos, Spain. Tel.: +34 947040800.
E-mail address: david.dominguez@cenieuh.es (D. Domínguez-Villar).

temperature has also been incorporated in speleothem modelled proxies (e.g., Kaufmann, 2003; Oster et al., 2010). Additionally, the calibration of temperature-dependent proxies from speleothems with external climate has been conducted (e.g., Frisia et al., 2003; Treble et al., 2003; Mangini et al., 2005; Baker et al., 2007; Matthey et al., 2008; Cai et al., 2010; Jex et al., 2011). Regardless of whether the interpretation of a particular speleothem record is linked to SAT or any other climate/geochemical variable, thermally dependent proxies will be affected by the changes in cave temperature. Therefore, a decoupled and variable relation between mean annual SAT and cave temperature could affect the speleothem calibration and the proxy interpretation.

Despite the great importance of cave temperature for the interpretation of many speleothem proxies, there are a limited number of studies focused in the coupling of cave temperature and SAT (Perrier et al., 2005; Genty, 2008). Although there are some studies connecting cave temperature and SAT (e.g., Moore and Nicholas, 1964; Smithson, 1991), little attention has been paid to the mechanisms transferring the temperature signal to the cave, and the time that takes for the cave temperature to respond to changes in SAT. Lag times in the hydrology of the cave systems are already considered when transferring the external signals to the cave for calibration purposes (e.g., Jex et al., 2010) or in models (Baker and Bradley, 2010). However, the lag time between changes in SAT and its record in caves, as well as the impact that those changes would have on speleothem proxies, is still unexplored. Additionally, it is well known that ground temperature at the surface depends not only in SAT but on its vegetation cover (e.g., Munroe, 2012). Changes in vegetation cover over caves can be natural or anthropogenic in origin, and the process being gradual (e.g., afforestation) or rapid (e.g., fire). A decoupling of SAT and cave temperature as a result of changes in the vegetation cover was not previously identified.

In this paper we focus on Eagle Cave in central Spain. A decrease of cave air temperature of the order of ~ 2 °C since the mid-1970s allows us to investigate the causes of this temperature change and the transfer mechanisms into the cave. A thermal model was implemented to reconstruct the cave air temperature for the last decades accounting for SAT and vegetation cover changes, incorporating the lag times resulting for thermal transfer from the surface. Finally, a synthetic $\delta^{18}\text{O}$ speleothem record is presented to evaluate the impact of cave temperature changes related to variations in the vegetation cover.

2. Cave air and ground temperature: theoretical background

Temperature is an easily measurable parameter of cave microclimate (Cigna, 1961; Eraso, 1962; Moore, 1964). For most studied caves, the air temperature far from the entrance is relatively stable during the year (e.g., Moore and Sullivan, 1978). In the cave entrance, the external and inner cave temperatures interact along a certain relaxation length, whose extension depends on local cave factors as the dimensions of galleries, air velocity and flow regime (Wigley and Brown, 1971, 1976). For those caves in which sections far away from the entrance record non-stable temperatures during the year (e.g., annual variability > 1 °C), the causes are usually related to the forced cave ventilation (e.g., Cropley, 1965; De Freitas and Littlejohn, 1987; Smithson, 1991; Pflitsch and Piasecki, 2003) or the thermal anomalies driven by water streams crossing the cave (Kranjc and Opara, 2002). It has been assumed that the stable temperature in caves is close to the mean annual SAT over the cave (Moore and Nicholas, 1964; Wigley and Brown, 1976; Moore and Sullivan, 1978). Thus, caves located at higher elevation and/or latitudes are normally cooler, in accordance with their mean annual SAT (Moore and Nicholas, 1964; Buecher, 1999). However, there are

many exceptions to this general assumption, and caves out of thermal equilibrium with their relative mean annual SAT are common, having differences of several degrees, with the caves either cooler (Myers, 1962) or warmer than the mean annual SAT (Atkinson et al., 1983; Buecher, 1999). Causes for the thermal differences between cave and mean annual SAT are not very well understood, since complete thermal evaluation of cave systems are scarce (Luetscher et al., 2008). However, underground temperatures in karst and non-karst areas are also studied in anthropological cavities such as mines, quarries, tunnels, wine cellars (Perrier et al., 2001; Salve et al., 2008; Mazarrón and Cañas, 2009), or in borehole and soil temperature depth-logs (e.g., Pollack and Huang, 2000; Smerdon et al., 2006), providing further general knowledge about the underground thermal dynamics.

The underground temperature depends on the heat transferred. Apart from rare cases with a local radioactive heat source, for most sites the underground heat sources in the upper crust are the geothermal energy and the heat provided from the atmosphere at the surface (Pollack and Huang, 2000). In the case of caves, human or other organisms can provide additional sources of heat (e.g., Cigna, 1993). Additionally, due to the high humidity levels in caves, latent heat effects during phase changes modify the energy balance impacting cave temperature (De Freitas and Schmekel, 2003; Luetscher et al., 2008). The study of deep borehole and soil thermal profiles has demonstrated that the transfer of heat within the subsurface is mostly due to conduction (e.g., Pollack and Huang, 2000; Smerdon et al., 2006). The geothermal gradients are relatively constant for a specific region and typical values range from 2.5 to 5 °C/100 m (Anderson, 2005). Above a certain depth, generally ranging from 150 to 50 m (e.g., Stevens et al., 2008), the geothermal gradients are modified because of the progressive importance of the atmosphere at the surface as a heat source/sink. However, due to the high permeability of the limestone rocks, the karst terrains present a different thermal pattern. The geothermal heat is drained by the aquifers due to lateral advection, and unless in those aquifers with stagnant water or limited flow, has little or no impact on the unsaturated zone of the karst (Bögli, 1980; Anderson, 2005). Thus, the thermal gradient in the deep vadose sector of karst terrains reflects the impact of water percolation through the high permeability of the rock. Because of the friction of water along the flow path, the rock is progressively warmed with depth and the thermal gradient is typically 0.2–0.4 °C/100 m (Badino, 1995; Luetscher and Jeannin, 2004). This gradient is slightly lower than the range of adiabatic gradients on the atmosphere at the surface, and the temperature measured deep in the vadose zone of a karst massif is often cooler than that found in the surface at the same elevation (Badino, 2005).

Many caves record seasonality in their temperature records due to advection or conduction of the SAT signal (e.g., Sánchez-Moral, et al., 1999; Spötl et al., 2005; Boch et al., 2011). Seasonality due to advection normally causes sudden and sharp thermal changes which are related to cave ventilation that responds quickly to meteorological changes at the surface (e.g., Smithson, 1991; Pflitsch and Piasecki, 2003; Bourges et al., 2006). The contrasting air-density between the cave and the exterior due to thermal difference of the atmosphere environments may produce a dynamic ventilation regime in some caves, which imprints a thermal seasonality due to heat advection (e.g., De Freitas and Littlejohn, 1987). In these cases, high-frequency oscillations in temperature accompany the seasonal signature. The seasonal cycles that transport the external temperature signal through the rock by conduction have a very regular sinusoidal signal (e.g., Sánchez-Moral, et al., 1999; Buecher, 1999). The amplitude of the thermal seasonality is muted with depth and there is a phase shift in relation with the SAT, the deeper the site the larger is the signal delay (Labs, 1982;

Smerdon et al., 2004). The thermal cycles driven by conduction of external seasonal temperature are completely muted below a certain depth, generally around 20 m (Pollack and Huang, 2000; Beltrami, 2001), whereas the thermal seasonality driven by advection does not have such depth-limitation. However, it is common for the thermal signal in shallow caves to record seasonality resulting from the combination of thermal conduction and advection transport mechanisms (Domínguez-Villar, 2012). The heat contained in a certain volume of karst rocks is ~1800 times larger than the heat found in the same volume of cave air (Pflitsch and Piasecki, 2003), and consequently for most cases, the long term temperature of the cave is controlled mainly by that of the rock walls (Wigley and Brown, 1976). In order to counteract the cave walls heat capacity by atmosphere advection, a dynamic cave ventilation able to displace large volumes of air is required (e.g., air mass interacting with the rock walls has to be more than ~1800 times higher than the rock mass considered, accounting for the rock wave vector). However, caves which air temperature is governed by heat advection from the surface are not uncommon (e.g., De Freitas and Littlejohn, 1987; Spöltl et al., 2005). The rock temperature in the shallow vadose zone of karst terrains (i.e., <20 m in depth) is dominated by heat conduction of ground surface temperature, with a minor influence of heat advection due to air and water flow (Badino, 2005). Therefore, the SAT signal, linked with the ground surface temperature, and then transferred to caves in this shallow vadose zone by conduction through the bedrock is thought to be the principal connexion between the observed stable cave temperatures and the mean annual SAT (Domínguez-Villar, 2012).

3. Eagle Cave environmental setting

Eagle Cave is located in the province of Ávila, central Spain, at coordinates 40°9'15"N, 5°4'20"W (Fig. 1). The cave is under a small (~0.11 km²) hill composed of dolomites which are concordant at the top of a series of metasediments (schist with occasional quartzite beds) of Cambrian age (Martín Escorza, 1971). The dolomites were affected by the intrusion of a granite stock during the Hercynian Orogeny (Odrizola et al., 1980) forming a skarn with iron oxides (Martín Escorza, 1971). The hill summit altitude is at 427 m asl (above sea level) and is bounded by two creeks (Avellaneda and Arenas) in its northwest slope. The creeks drain towards the Tietar River that flows parallel to the hill 500 m to the

southeast at an elevation of 365 m asl. A meteorological station recently installed at the base of the cave hill has a record of three complete years (2009–2011). During this period the mean annual SAT was 14.8 °C (mean January and July SAT are 5.9 and 24.9 °C respectively) and the mean annual total amount of precipitation was 797 mm. Due to the low altitude of the cave site, the average number of freezing days per year is limited (45 days), and the snow rarely covers the ground, melting down within a day. The precipitation has a distinct maximum during the winter, and a summer drought (i.e., monthly rainfall <20 mm) lasts for 3–4 months. The soil over the cave consists of a rendzina with a variable depth (0–>0.5 m) due to irregular rock exposures. The dolomite hill has an evergreen oak forest canopy (<4 m tall) with an undergrowth of shrubs that makes it difficult to traverse (the place is known as the “ripping clothes hill”). Nowadays, clearances in the forest are rare and mostly related to small quarries. However, the hill vegetation has been subject to substantial changes in the past decades, and trees were rare in the hill some decades ago as observed in historical pictures. According to testimony of local people a fire affected the cave hill before the year 1946, although the absence of forest above the cave during decades after (and maybe before) the fire, might wholly or in part be related to intense land use in the past (i.e., wood-gathering) by local farmers.

Eagle Cave was discovered in 1963, and has operated as a tourist cave since 1964. Since its discovery, two solid wooden doors, close to each other and located at the same elevation, were used to enter and exit the cave (Fig. 1). At the entrance/exit, two parallel 30 m long galleries descend by a moderate slope for ~10 m until the main cave hall is reached. The hall is a collapse room with the ceiling at 5 m from the cave floor on average. The lowest altitude of the hall is at the connexion with the entrance/exit galleries, and the distal sections of the cave are generally close to the entrance elevation. Several small galleries are connected to the main hall, although none of them has a known connexion to the surface or deeper levels of the karst system. However, when the different galleries are included, the altitude range within the cave is >20 m. A lighting system was installed when the cave was discovered, consisting in a series of 200 W bulbs spread out along the cave. This lighting system was replaced by a cold-light illumination system in 2008 just before our monitoring programme in Eagle Cave started. When the cave was equipped for tourist exhibition, an air extraction system was installed (air is suck out), and since then the cave is vented daily for 1.5 h. A record of the cave temperature was conducted during 3 yr from 1973 until 1976, under the supervision of the mining engineer Juan Pantoja. The data were kept by the cave managers, but were never published. The temperatures were taken with an analogue psychrometer and the readings considered only integer numbers even when the device allows a better precision. The temperature values were acquired daily prior to the first morning visit of the tourists. The data were recorded only during the first half of every month, providing a discontinuous but consistent sampling dataset. The readings were systematically taken by the same operator (Mr. Jorge Gómez) and were quick, to avoid impacting the environmental temperature (since the logger responds significantly to the operator presence after >10–20 s). The cave temperature record showed a constant temperature of 18 ± 0.5 °C (uncertainty accounting for half the precision reported) and a relative humidity of $100 \pm 5\%$ during the monitoring period.

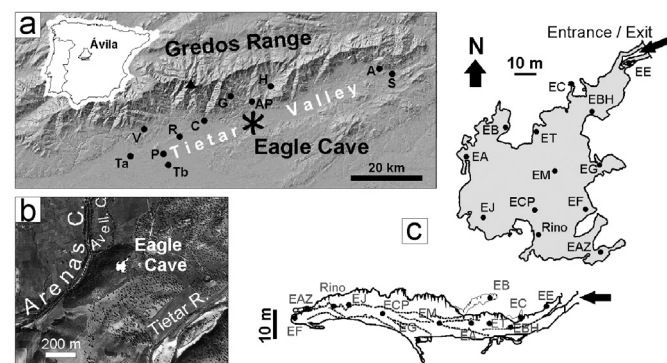


Fig. 1. Location and cartography of Eagle Cave. (a) Situation of Tietar Valley in the Iberian Peninsula and location of the meteorological stations from the AEMET database in the valley. For codes of the meteorological stations see [Supplementary material](#). The location of Eagle Cave is indicated with an asterisk. The triangle shows the highest summit of the Gredos Range at Almanzor Peak (2592 m asl). (b) Aerial photograph from the cave hill and its surroundings showing the fluvial network. The cave plan is shown over the hill. (c) Map and profile of Eagle Cave (after Villaverde et al., 2009), with the location of the thermometers used in this study.

4. Methods

Cave temperature was measured with 13 Tiny Tags TGP-4017 and TGP-4500 equipped with 10 K NTC thermistors from November

Table 1
Eagle Cave temperature measured in selected sites from November 2008 on.

Site code	Cave location	Logger type	Duration of the record (d)	Average temperature (°C)	Thermal amplitude (°C)
EE	Entrada	TGP-4500	1107	15.06	3.17
EBH	Búho	TGP-4500	280	15.55	0.19
EC	Chimenea	TGP-4500	903	15.24	0.47
ET	Tortuga	TGP-4017	503	15.66	0.27
EM	Mazorca	TGP-4017	640	15.65	0.31
EB	Barrizal	TGP-4017	293	15.68	0.18
EA	Águila	TGP-4500	381	15.63	0.12
ECP	Columna partida	TGP-4500	510	15.64	0.31
EJ	Jardín	TGP-4500	255	15.80	0.32
EG	Grieta	TGP-4500	625	15.54	0.17
Rino	Rinoceronte	TGP-4017	1240	15.80	0.53
EF	Fondo	TGP-4017	497	15.64	0.31
EAZ	Azahar	TGP-4017	631	15.53	0.47

2008 onwards (Table 1). The thermometers provide an output reading of 0.001 °C (i.e., precision of ± 0.0005 °C) and their accuracy is better than 0.5 °C. The logger reproducibility was tested inside the stable environment of the cave. The loggers were deployed in a gallery that is known to lack any daily thermal variation and left for a day to allow the thermal signals to be stabilized. According to this test, the temperature signal reproducibility of the loggers is ± 0.04 °C. The loggers were deployed over the cave ground in different sections of the cave and programmed to measure temperature at 10 min intervals. In one of the measuring spots (EM) an additional logger was set over a tripod at 100 mm from the cave floor. The logger at the tripod records higher oscillations during the day (maximum differences are ± 0.02 °C) although the average difference in the filtered daily temperature between both thermometers, which is the data considered in this paper (see below), was 0.007 ± 0.003 °C, clearly within the reproducibility uncertainty. During the monitoring period, several sensors had problems with humidity and temperature signals drifted. The periods with unreliable records have been eliminated. Soil temperature was measured with Tiny Tag loggers similar to those used inside the cave. These loggers were calibrated inside the cave before being buried. Three sections of the hill or its surroundings presenting different vegetation cover were selected to quantify the effect of their canopy in the surface ground temperature. The loggers were buried 0.5 m under (1) the forest over the cave, (2) a sector dominated by shrubs and (3) a parcel covered with grass. The soil temperatures were recorded hourly. Surface air temperature was measured together with other parameters in a Vaisala WXT510 meteorological station. The station is equipped with a Thermocap sensor that provides an accuracy of ± 0.3 °C and an output reading of 0.1 °C (precision ± 0.05 °C). Temperature is measured at 2 m above the ground, in a flat prairie terrain, near to the cave (i.e., 75 m from cave entrance). The SAT in the meteorological station was measured at 10 min intervals. An evolution of the regional temperature was obtained using 11 meteorological stations in the Tietar Valley from the Spanish meteorological stations database (AEMET). The temperature record begins from 1954 AD and three stations are still operative (see Supplementary material).

To study the thermal diffusion of temperature by conduction, the depth of the cave needs to be known in detail. A topographic map of the cave was conducted (Villaverde et al., 2009), using a clinometer and a laser beam incorporated in a tripod. The error in the distance of the horizontal and vertical readings was better than 0.01 m and the average error in the polygonal ($n=15$) was 0.22%. Each of the measurement stations considered to produce

the cartography included not only horizontal distances but the ceiling height (stalactites were avoided). The topography of the cave hill was obtained from a 10 m equidistant nodes grid, measured with a differential GPS with horizontal and vertical errors of ± 0.005 m and ± 0.01 m respectively. The cave topography was anchored to the coordinates and elevation at the entrance of the cave that were measured with the differential GPS. Thus, cave and surface topographies have a similar reference point. The bedrock thickness over the cave was calculated subtracting the elevation of the surface topography and the cave ceiling with an estimated error of ± 0.5 m. To study the vegetation cover evolution over the hill aerial photographs of scales 1:20,000–1:40,000 were investigated. The series of images includes the years 1946, 1956, 1977, 1984, 1996, 1999, 2002 and 2010, and were obtained from the Spanish Army, National Geographical Institute, and Ministry Agriculture archives. Density of forest cover over the cave was estimated from each image and a continuous annual series of density of forest cover was obtained interpolating data between known dates.

Eagle Cave is visited by tens of thousands of tourists every year, which causes temperature changes to the cave air. As the tourists pass by the entrance/exit galleries and the main hall, their thermal footprint is limited to those sections, and some galleries do not record any tourist influence. The thermal impact of visitors in the cave is transitory and normally last less than a day. Thus, the natural cave temperature can be calculated from the recorded signal after filtering the tourist thermal anomalies (Domínguez-Villar et al., 2010). The forced venting of the cave also produces daily anomalies in two loggers located close to the entrance and in a corridor. After filtering these main thermal anthropogenic anomalies by selecting specific daily periods for each logger in which anthropogenic impact is minimum or non-existing, the mean daily temperature was calculated.

5. Results and discussion

5.1. Tietar Valley and Eagle Cave air temperatures

In contrast with what it is observed in most Spanish temperature records (Brunet et al., 2007), no global warming trend is recorded in air temperature archives from Tietar Valley. In this region the temperature has been stationary for the last 19 yr, with an average SAT of 15.4 ± 0.2 °C ($n=3$; sites S, R and P in Fig. 1). The mean annual SAT varies by several degrees among different locations. These thermal differences cannot be attributed to the altitude effect and local effects contribute to the SAT in each location. However, anomalies seem to be common for the region, and a normalized composite record of mean annual SAT in the Tietar Valley has been carried out (Fig. 2), considering 1954–2011 as the normalization period. The mean temperature measured in Eagle Cave from November 2008 until March 2012 was of 15.6 ± 0.2 °C, with a maximum thermal difference between loggers of 0.7 °C (reproducibility of temperature values from these two particular loggers was better than 0.01 °C). The cave temperature recorded is very close to the regional mean annual SAT (15.4 °C), although is slightly warmer than the local mean annual SAT (14.8 °C), measured from 2009 until 2011 in the meteorological station outside the cave. This difference is not surprising due to the limited period of record of this station and the large inter-annual variability (up to 0.8 °C). These data indicate that the cave temperature is in equilibrium within 1 °C with the mean annual SAT. In order to refine the evaluation of the thermal equilibrium of cave with the local mean annual SAT, a longer record outside the cave (several additional years) is required.

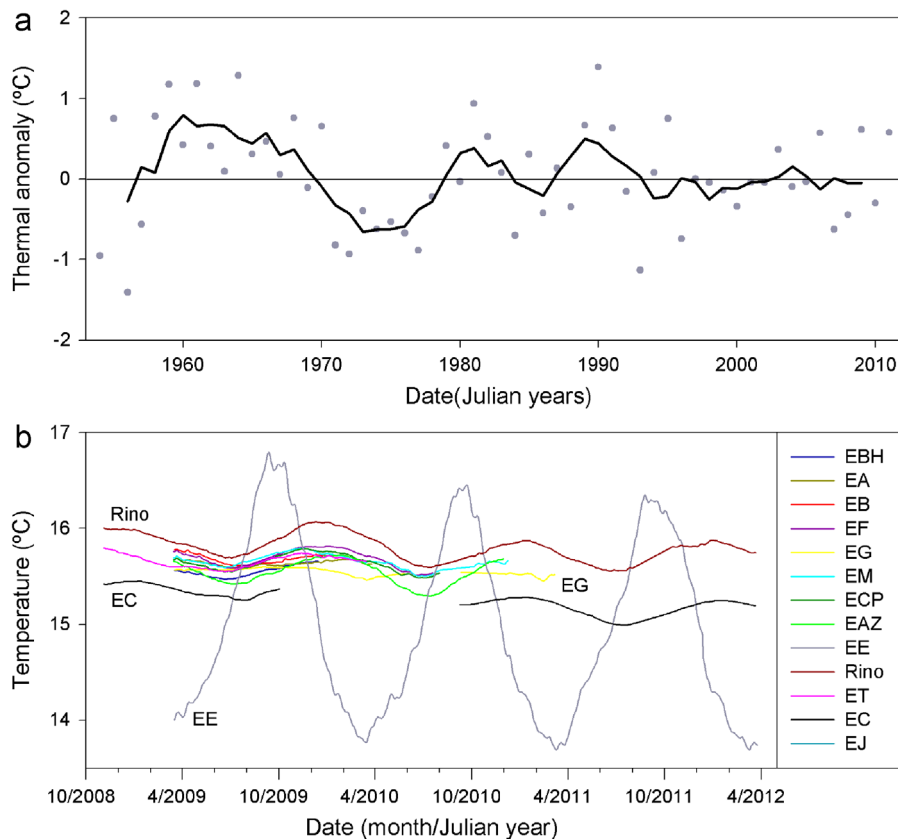


Fig. 2. Temperature records. (a) Thermal anomaly of the mean annual SAT over the region of Tietar Valley from 1954 to 2011. The full period of record was used for normalization. Bold line represents a 5 yr moving average. (b) Daily cave temperature with a 7-day pass filter from November 2008 until March 2012 in Eagle Cave. Temperature records referred in the text are labelled.

All the cave records show seasonality in the temperature signal (Fig. 2). The logger located closer to the surface (EE) records the largest thermal amplitude (of the order of 2.4 °C), whereas the rest of the records show amplitudes < 0.5 °C. All the thermal signals follow a roughly sinusoidal pattern. There are cases in which the sinusoidal cycles are suddenly disrupted, as in the EG site. In contrast, the site EC shows almost perfect sinusoidal cycles for most of its record. The small amplitude and high frequency perturbations of the signal result from residuals remaining after the removal of the thermal footprint of tourists. In the case of EE, the high frequency perturbations are the result of persistent thermal anomalies after the daily artificial venting of the cave, and they are more pronounced during summer and winter months. Additionally, there is a phase shift of the sinusoidal cycles of thermometers located in different galleries (e.g., EE, EC, EG), suggesting that the sinusoidal pattern is the result of heat conduction through the bedrock. However, during the clear disruptions of the sinusoidal pattern, that occur in some records during part of the year, advection dynamics dominate the signal. It is obvious in the EG record for example, that during spring there are some weeks/months of substantially lower temperatures. The mean temperature of the logging sites in the main hall of the cave present differences of 0.3–0.4 °C from the warmer to the cooler site. Additionally, all the sites display roughly in-phase seasonal oscillations regardless of the differences in thickness of bedrock above them. This suggests that advection of air within the main cave hall is redistributing the temperature provided by the cave walls, even when there are no measurable air currents. Higher temperatures within the hall are observed at higher elevations ($r^2=0.49$, $p=0.016$), indicating the importance of cold traps and warm pockets (cf. Luetscher et al., 2008; Pflitsch and Piasecki,

2003). Thus, advection within the main hall is redistributing the heat provided by its ceiling and walls, homogenizing the seasonality of the records and causing some thermal differences related to elevation and/or micro-topographical constraints. Thus, the advection detected in the main hall is the result of the topographic differences and is independent from flows between the exterior and the cave. So, although we are aware that some advection takes place in the main hall, it only redistributes the heat provided by the conduction through the bedrock, which dominates the mean temperature recorded in the cave.

5.2. Evaluation of the temperature monitoring from the mid-1970s

Temperature was measured in Eagle Cave from July 1973 until August 1976 with an analogue psychrometer. During this period the temperature was constant at 18 °C, with only one exception, 17 of May 1975, in which the temperature was 17 °C. Only integer numbers were considered even when the thermometer allows a better precision (i.e., ± 0.1 °C). The same psychrometer that was used in the 1970s was kept by the cave managers after the experiment concluded. So, we deployed the original psychrometer together with one of our thermistors at the same location where the 1970s record was obtained: the “Rino” site. Comparison of single readings ($n=13$) from the two thermometers during a period longer than 2 yr demonstrated that the old psychrometer provides readings 0.6 ± 0.1 °C warmer than the thermistor. This thermal offset was stable during the period of calibration. Due to the excellent conservation state of the psychrometer, there are no reasons to think that its mercury capsule could have suffered any damage or deterioration causing an offset of temperature through time. So, the offset between loggers is considered to be the result

of the devices accuracy differences and to have been stable through time. The temperature at Rino site measured with the thermistor from November 2008 until March 2012 was 15.8 °C. In order to compare the thermistor record with the old psychrometer record, the thermal offset identified during the calibration is added to the thermistor (16.4 °C) and then only the integer number is considered: 16 °C. Therefore, a cave cooling in the order of 2 °C should be considered, with an uncertainty of ± 0.5 °C that accounts for half of the significant digits reported.

The cave has been open to tourists since 1964, and tens of thousands of people visit the cave every year. The cave air temperature increases with the number of visits, although their footprint is frequently ephemeral and, in most cases, the pre-visit temperature recovers overnight (Domínguez-Villar et al., 2010). With large number of visitors per day (i.e., several hundreds) the temperature is not completely recovered before the visits of the next day, although cumulative thermal anomalies are < 0.1 °C and they recover shortly after the number of visitors decrease (Domínguez-Villar et al., 2010). Thus, the effect of current number of visitors for the long-term cave temperature is negligible, and the number of visits during the past four decades was in the same order of magnitude according to cave managers. Therefore, the impact of tourist in Eagle Cave should not be considered to evaluate long-term cave temperature trends. However, the lighting system of the cave was modified in 2008 just before the current monitoring period started. Because the new cold light illumination system could account for some temperature decrease in comparison with the previous lighting system, an experiment was conducted to evaluate the temperature that the 200 W bulbs (old lighting system) were yielding. One of the illumination points is set ~ 2 m apart from Rino site, although the thermometers are behind a large speleothem. In this lighting site, temperature was measured with two additional thermistors at 0.5 and 1.1 m from the cold light source. After several days of the experiment, the light was replaced by a 200 W bulb in identical conditions as they were set in the past, and left for three days. The results indicate that at 0.5 m from the light source, the 200 W bulb yielded a 3.7 °C thermal anomaly, whereas the cold light cause a 0.3 °C warming. The thermal anomaly at 1.1 m from the light source is only 0.3 °C with the 200 W bulb and negligible with the cold light (< 0.04 °C). At Rino site, the effect of both lighting systems is negligible (see Supplementary material). For both illumination systems, shortly after the lights are turn off, the temperature reach the pre-illumination temperature values. The electrical energy used by both lighting systems to generate the light produce heat. The positive thermal anomalies caused by the lights are the result of sensible heat produced by the lighting sources, and their impact are muted in < 2 m for the 200 W and < 1 m in the cold light illumination system. The evaporation of moisture causes cooling of the cave air (Atkinson et al., 1983). Evaporation can occur even with cave air saturated in moisture since the moisture-holding capacity of air increases with temperature (De Freitas and Schmekal, 2003). Thus, the latent heat is the most likely responsible mechanism for muting the thermal impact of the lighting systems in a short distance. As the space between lights spots is much larger than the ratio needed to mute the thermal anomaly they produce, both illumination systems produce a local impact that does not affect the general cave temperature. In any case, the thermometers at Rino site are out of the perimeter affected by any light source. Therefore, the change in lighting system cannot account the thermal cooling recorded after mid-1970s.

5.3. Calculation of the thermal diffusion coefficient

Considering the limited effect of advection in the recorded mean cave temperature, and the negligible thermal impact of the visitors

and the lighting system for the long-term evolution of the cave temperature, the conduction of the ground surface temperature through the rock is expected to be the dominant factor for the long-term cave temperature changes. Considering a homogeneous, semi-infinite source-free half-space the conduction of temperature along one direction is governed by the heat diffusion equation (Carslaw and Jaeger, 1959)

$$\frac{\partial T}{\partial t} = \kappa \frac{\partial^2 T}{\partial z^2} \quad (1)$$

where T is the temperature measured in °C at time t (in s) and depth z (in m), and κ is the thermal diffusivity expressed in $\text{m}^2 \text{s}^{-1}$. The value of κ is considered constant and normally taken from tabulated values for different materials (Cermak and Rybach, 1982). However, for detailed calculations, especially at shallower depths where ground properties can differ substantially (e.g., soil representing a substantial percentage of the depth under consideration, rock weathering affecting porosity and permeability, differential moisture content, etc.), the calculation of the local κ is desired (e.g., Beltrami and Kellman, 2003; Smerdon et al., 2006). Calculation of κ can be obtained from phase lag or thermal amplitude at different depths (Smerdon et al., 2003). The phase shift of the thermal cycles is *a priori* unknown in the cave, since a continuous vertical thermal profile is lacking and the observed shifts of the thermal cycles in relation to SAT are expected to be delayed for an unknown number of years (Domínguez-Villar, 2012). Therefore, the calculation of Eagle Cave κ was conducted from thermal anomalies at different depths. To do such analysis a good calculation of the bedrock thickness over the cave ceiling is needed. In Eagle Cave the thickness of the bedrock over cave was calculated subtracting the cave ceiling and surface topography (Fig. 3a). Thus, the bedrock thickness over each thermometer can be estimated with a precision better than 0.5 m. Five records were selected to calculate the κ , including the external thermometer and a thermometer buried at 0.5 m under the forest over the cave. The selected temperature records inside the cave are from different galleries to avoid any advection modification of the thermal amplitude.

The value of κ can be calculated knowing the wave vector (k) according to the equation

$$k = \sqrt{\frac{\pi}{\tau + \kappa}} \quad (2)$$

where τ is the period measured in s. The wave vector is calculated from the slope of the linear relationship between the natural

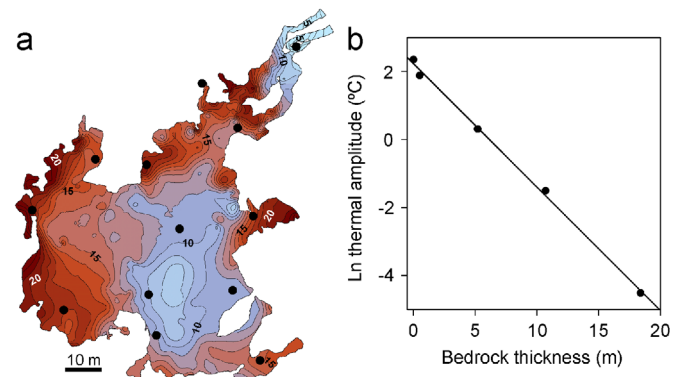


Fig. 3. Bedrock thickness on top of Eagle Cave and its thermal diffusion coefficient. (a) Map of the thickness of bedrock cover over the cave. Contour lines are drawn each metre and labels indicate the bedrock thickness each 5 m. The dots indicate the location of the thermometers. See Fig. 1 to identify the logger codes. (b) Cross-plot of the thickness of bedrock/soil from the thermometer to the surface versus the natural logarithm of the thermal amplitude at each site. The slope of the graph is related to the wave vector (k), a parameter that is used to calculate the thermal diffusion coefficient (κ) according to Smerdon et al. (2003).

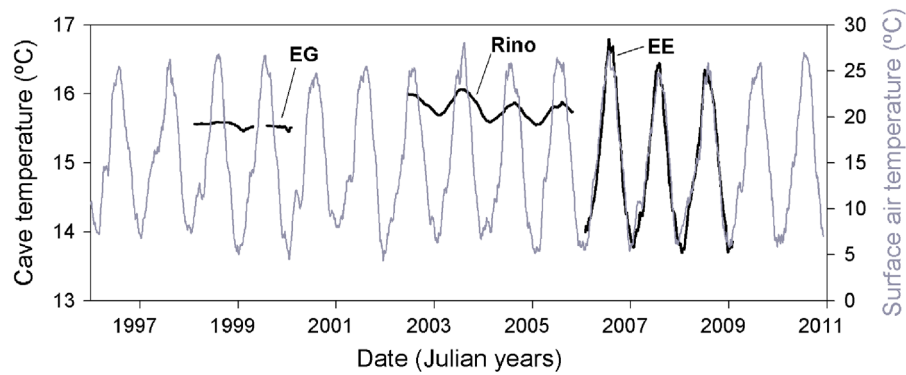


Fig. 4. Comparison of surface air temperature at Pantano de Rosarito station with Eagle Cave temperature signals from three different galleries when their records are shifted back in time according to the calculated phase shift from the thermal diffusion coefficient (κ). Note that the dates represent a real time scale only for Pantano de Rosarito. The lag time between the plotted cave temperatures and the real time scale represents the time required for the SAT to reach each gallery. Thus, the galleries with the thicker bedrock cover above the ceiling record a temperature related to the SAT from earlier dates than the galleries with thinner bedrock cover.

logarithm of the thermal amplitude (i.e., semi-amplitude) at each site and the depth (Smerdon et al., 2003, 2004). Thus, the wave vector empirically calculated for Eagle Cave ground (i.e., including rock, soil and fluids) from Fig. 3b provides a κ of $0.756 \times 10^{-6} \pm 0.013 \text{ m}^2 \text{ s}^{-1}$. Once κ is known the phase shift (ϕ) can be calculated (Smerdon and Stieglitz, 2006) according to

$$\phi = \kappa \cdot Z \quad (3)$$

Fig. 4 shows the fit of three cave temperature records from different galleries when they are shifted back in time according to Eq. (3), in comparison with the daily temperature record of the meteorological station from Pantano de Rosarito, which is 22 km distant from the cave. At EE site, where the bedrock thickness to the surface is ~5 m, the lag time is over 3 yr ($r^2=0.95$, p -value < 0.001). At Rino site that has a bedrock thickness over the ceiling in the order of 11 m the delay exceeds 6 yr ($r^2=0.61$, p -value < 0.001), and in EG site with ~18 m of dolostones above the delay is near 11 yr ($r^2=0.39$, p -value < 0.001). The decreased correlation factor with time is the result of assuming a constant value for κ and of propagating the uncertainty through the calculations. The good fit of cave temperatures with the surface air temperature record confirms that the downwards conduction of the external temperature is responsible for most of the recorded thermal variability. The sites that have a thicker bedrock cover above them show smaller thermal amplitudes and larger phase shifts. The phase shift represents the time that the external temperature signal takes to reach the cave at the depth of a particular gallery.

5.4. Cave thermal models

5.4.1. Thermal impact of the surface air thermal anomaly during 1960s in the cave

The SAT signal takes 6–7 yr to reach the main hall of Eagle Cave by thermal conduction. Thus, the higher temperatures measured in Rino site from 1973 until 1976 in relation to the present could be related to any thermal anomalies recorded in the Tietar Valley during the 1960s (Fig. 2). The thermal amplitude and duration of the positive thermal anomaly in 1960s in Tietar Valley slightly varies in the different meteorological stations. During this period, some meteorological stations in the valley record positive anomalies 1 to 2 °C warmer than their record average, whereas others have 0–1 °C positive anomalies. A cooling trend began in 1969 AD for most of the stations in the valley completing the positive thermal anomaly that lasted approximately a decade. However, when transferring transient temperature changes underground, the recorded thermal anomaly would be muted in relation to the external signal. To calculate the expected increase in cave

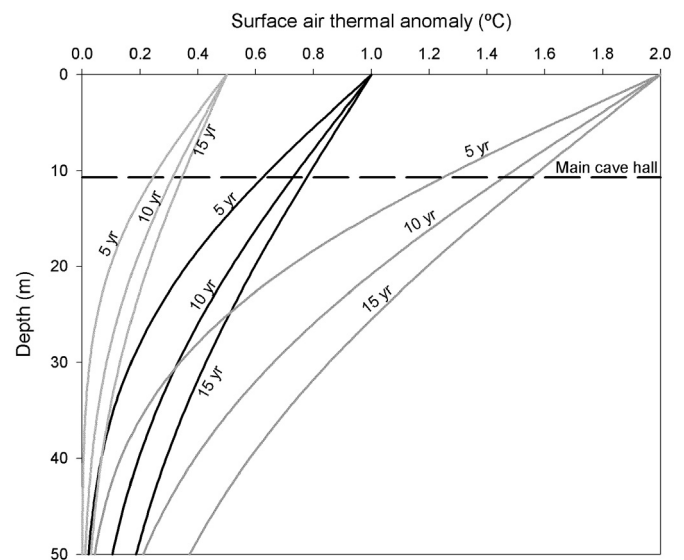


Fig. 5. Graph showing the thermal conduction of SAT anomalies of 0.5, 1.0 and 2.0 °C underground considering the Eagle Cave κ value. The duration of 5, 10 and 15 yr for the thermal anomalies are considered. The mean depth of the ceiling in the main hall of Eagle Cave is indicated with a bold horizontal line.

temperature caused by an anomaly in mean annual SAT we used the solution of Eq. (1) given by Stevens et al. (2008),

$$T = T_0 \operatorname{erfc} \left(\frac{z}{2\sqrt{\kappa \cdot t}} \right) \quad (4)$$

where T is the temperature recorded underground, and T_0 represents the thermal anomaly in °C. Considering the κ value calculated for Eagle Cave, a thermal amplitude of 1.0 °C lasting 10 yr, would produce a temperature increase of 0.73 °C in the main hall of the cave (Fig. 5). Even when considering slightly different durations and amplitudes of the surface air thermal anomaly, it is clear that its conduction is insufficient to explain the observed cave temperature difference between present and the mid-1970s temperatures. Therefore, additional factors should be considered to properly model the cave temperature.

5.4.2. Ground surface temperatures and cave temperature reconstruction

Because ground and air temperatures are expected to be coupled (e.g., Smerdon et al., 2004; Pollack et al., 2005) the impact of changes in SAT are recorded in the cave. However, ground temperature does not depend exclusively in SAT, and other factors have been

considered, such as vegetation, snow cover, soil humidity, latent heat changes and solar radiation (e.g., Beltrami and Kellman, 2003). The snow cover clearly isolates the ground temperature during winter months (Smerdon et al., 2006) and changes in soil moisture due to extensive agriculture have modified ground temperatures over large regions (Stevens et al., 2008). None of those circumstances are applicable to Eagle Cave. Deforestation can cause several degrees of warming of the ground surface temperatures (Lewis and Wang, 1998; Nitoiu and Beltrami, 2005; Ferguson and Beltrami, 2006). Changes in the forest cover over Eagle Cave are known for the past decades. Regardless of the existence of the fire, the land use was modified after the cave was discovered, and the dense shrub canopy of the cave hill was replaced progressively by an evergreen oak forest with dense undergrowth. To test the effect of the local impact of vegetation on ground surface temperature we have selected three locations around the cave with different vegetation covers: grassland, shrubs and forest. The ground temperature on these locations differs considerably (Fig. 6), with the most pronounced contrast among the loggers in summer (>10 °C). Thermal differences on the mean annual temperature at the different sites produce: 1.87 °C between the forest and shrub sites, 3.27 °C between the forest and grassland sites, and 1.40 °C between the shrub and grassland sites.

The percentage of shrub versus forest cover over the cave can be estimated from successive aerial photographs taken over the cave. Considering the eight aerial pictures available for the cave site since 1946, we have reconstructed the percentage of forest cover (Fig. 7). A sharp increase in forest coverage is already obvious soon after the cave discover in the 1970s, when most of the trees began to grow. To evaluate the thermal effects of afforestation of the cave hill, the thermal difference obtained between shrub and forest cover (1.87 °C) is considered between 100% shrub and 100% forest end members. The increase of forest cover during the last decades should not cause a transient change to cave temperature but a progressive and persistent shift of the underground temperature. Thus, the signal of ground surface temperature is expected to be diffused and delayed in relation to the ground surface, but not muted. The changes in vegetation cover and the SAT are considered here to reconstruct the evolution of cave temperature at the Rino site for the past decades (Fig. 8a).

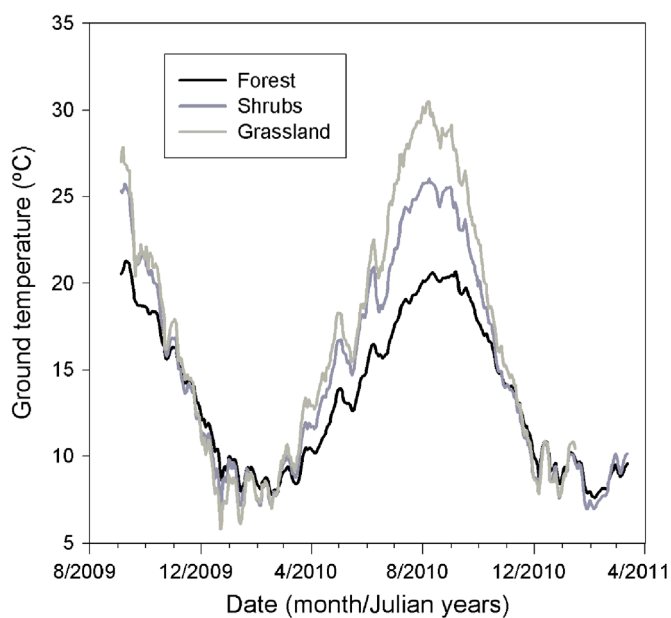


Fig. 6. Ground temperatures at three sites with different vegetation covers. The thermometers were buried 0.5 m under the surface. All the sites are close to the cave and the parent rock of the soil is dolomite rock as in the cave.

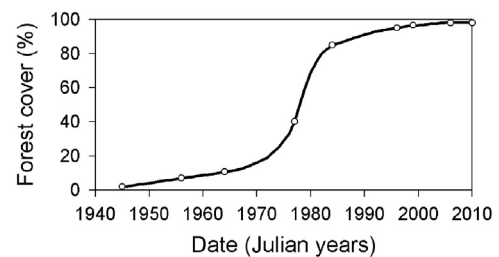


Fig. 7. Evolution of the percentage of forest cover over Eagle Cave. The white dots represent the data obtained from aerial pictures. The rest of the series was interpolated between data points. A knick point was introduced the year when the cave was open to tourist (1964 AD) as it is known that the land use of the cave hill was modified after this date.

It is obvious that the impact of afforestation on the cave hill is much more significant that the inter-annual variability of the mean annual SAT. However, conduction of temperature has shown that the variability of the mean annual SAT is being recorded in the cave. Therefore, both elements were considered for the cave temperature reconstruction at the main hall (Fig. 8b). The proposed cave temperature reconstruction agrees within the errors with the observations made in mid-1970s in the cave and can explain the decrease of ~ 2 °C of cave temperature at Rino site since then until today.

6. Implications for speleothem palaeoclimate

Most of the change in Eagle Cave temperature during recent decades is not related to climate but to changes in vegetation cover over the cave as a result of modification of the land use and/or the recover after a fire. In this case, there is a clear decoupling between SAT and cave temperature for the period of interest. This kind of thermal decoupling in caves can be of critical importance for palaeoclimate studies since, as discussed earlier, some of the most used speleothem proxies are temperature-dependent (Fairchild and Baker, 2012). Regardless whether the interpretation of these proxies is dominated by temperature or by other factors, the changes in cave temperature affects their signal. The existence of a variable thermal decoupling between the surface and the cave implies that the speleothem proxies record a variability not related to climate changes. Thus, a variable decoupling between SAT and cave temperature may affect the signal recorded in the speleothem independently to climate. The $\delta^{18}\text{O}$ proxy is the most commonly used in speleothem records (Fairchild et al., 2007), and we use it here as an example to illustrate the importance of cave temperature changes on the modification of the speleothem signal. Fig. 9 shows the $\delta^{18}\text{O}$ composition of a theoretical calcite speleothem precipitated under equilibrium conditions from a constant drip water isotope composition in Eagle Cave over the past decades. Although variations in drip water $\delta^{18}\text{O}$ composition at various timescales would be expected, the unrealistic scenario of a constant drip water isotope composition was chosen in order to focus on the impact that the temperature changes alone have in the $\delta^{18}\text{O}$ speleothem record. The use of the thermal reconstruction from Eagle Cave results in an unlikely $\delta^{18}\text{O}$ record, since SAT affect both rainfall $\delta^{18}\text{O}$ and cave temperature, and the drip water isotope composition would not be constant. However, changes in the forest cover do not affect the rainfall $\delta^{18}\text{O}$ and have a substantial impact on cave temperature. Thus, the $\delta^{18}\text{O}$ values in the synthetic record are 0.36‰ higher due to the afforestation effect occurred in the last decades. Considering that in most of the speleothems the $\delta^{18}\text{O}$ variability over the past five millennia is in the order of 1–2‰ (e.g., McDermott et al., 2011), the change in calcite oxygen isotopes

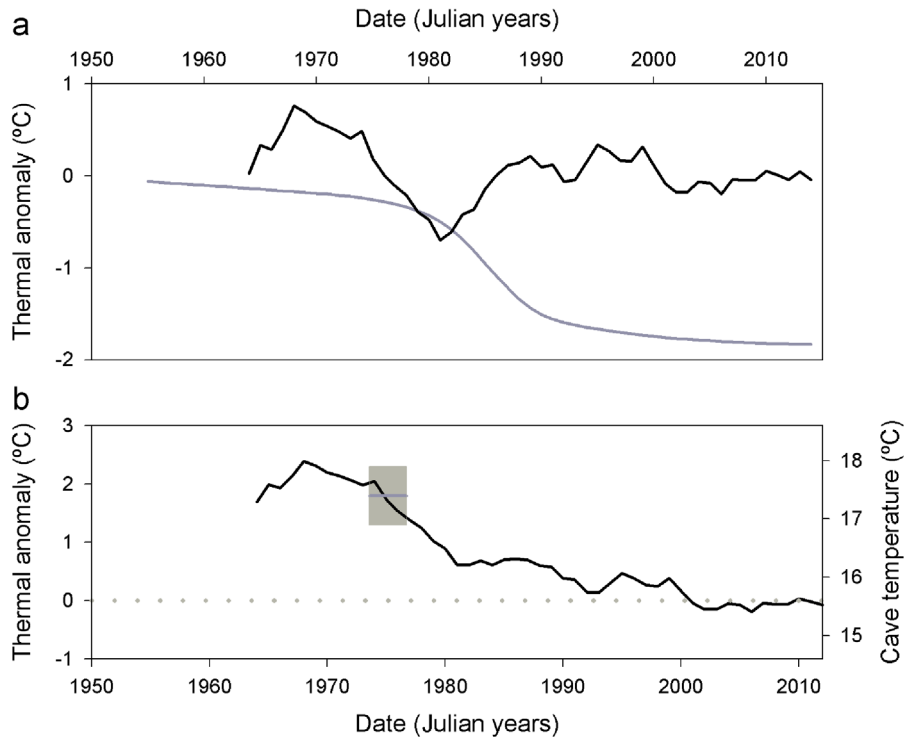


Fig. 8. Reconstructed mean annual thermal anomalies from Eagle Cave for recent decades. (a) Reconstructed thermal anomalies at Rino site due to changing cover of forest on the cave hill (grey line) and due to the changes in the mean annual SAT (black line). (b) Reconstructed mean annual temperature and thermal anomaly at Rino site during the past decades (black line) considering the effects of afforestation and the inter-annual changes of the SAT. The dark grey line shows the shift-corrected temperature during mid-1970s with its uncertainty as the grey box. The thermal anomalies are referred to the 2009–2011 period (grey dotted line).

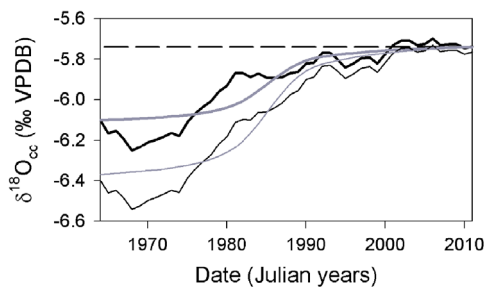


Fig. 9. Effect of the Eagle Cave temperature changes in a synthetic $\delta^{18}\text{O}$ calcite record (black bold line). The calculations consider a constant drip water composition (-6‰ SMOW) and equilibrium conditions according to Kim and O'Neil (1997). The dashed line shows the theoretical $\delta^{18}\text{O}$ composition of a calcite speleothem with constant cave temperature. The synthetic $\delta^{18}\text{O}_{\text{cc}}$ record that accounts only for the afforestation thermal effect in the cave (grey bold line) is responsible for an isotope enrichment of 0.36‰ . A hypothetical change from prairie to forest cover over Eagle Cave would cause larger modifications on the synthetic $\delta^{18}\text{O}_{\text{cc}}$ record (black thin line), with the impact of afforestation alone (grey thin line) having 0.63‰ higher values than the constant temperature scenario.

due to thermal decoupling is substantial. Potentially, the range of isotope changes due to vegetation cover may be even larger if a grass cover dominating the cave hill would have been progressively replaced by a forest (e.g., a deglaciation scenario). The impact on speleothem $\delta^{18}\text{O}$ values of such a change in vegetation cover in Eagle Cave during the last decades would be 0.63‰ higher after the afforestation regardless SAT changes. There are other factors affecting speleothem $\delta^{18}\text{O}$ records that cause even higher variability to the samples (e.g., rainfall $\delta^{18}\text{O}$ inter-annual variability), but the calcite fractionation in caves with variable thermal decoupling could be significant under particular circumstances and in those cases it should be considered together with

the other sources of oxygen isotope variability in order to properly explain the $\delta^{18}\text{O}$ speleothem records.

Recent speleothem $\delta^{18}\text{O}$ records have previously been investigated from an abandoned British mine over which a significant afforestation took place in the past decades (Baldini et al., 2005). The $\delta^{18}\text{O}$ records of three different speleothems from this cave show ^{18}O -depletions over the past half century. This trend is opposite to the expected due to the thermal effects of afforestation, and implies that in this case other factors dominate the $\delta^{18}\text{O}$ signal (Baldini et al., 2005). Examples of vegetation changes over caves in longer time scales have also been recorded. Shifts in the prairie/forest ecotone in north-central USA during the Holocene were described from speleothems and pollen analyses of land surface (Dorale et al., 1992; Denniston et al., 1999). In this case, during periods when there was a prairie over the cave sites, the oxygen isotope records of four speleothems in three different caves show values $1\text{--}2\text{‰}$ lower than during periods with a forest cover over the sites. These isotope trends are in agreement with the expected change caused by the modification of the decoupling between SAT and cave temperature. Considering the magnitude of the $\delta^{18}\text{O}$ shift in these speleothems associated with changes in vegetation cover, the thermal decoupling is likely to be a significant contributor of the observed isotope changes. These two examples illustrate that although the thermal decoupling control is unlikely to dominate the $\delta^{18}\text{O}$ record of speleothems due to the larger imprint of other factors, in particular cases with counteracting factors and/or reduced isotope variability in the system, it could explain a significant part of their variability.

The thermal decoupling between SAT and cave temperature may be the result of changes in vegetation cover, but it can be caused or contributed by other factors (Pollack and Huang, 2000; Beltrami and Kellman, 2003). Snow cover is an effective insulator preventing the record of temperatures below zero in the ground surface, resulting in warmer ground conditions relative to the

air (e.g., Vieira et al., 2003). The snow cover effect may account for even larger thermal decoupling compared to vegetation cover effect (Smerdon et al., 2006). Thus, the changes in duration of a significant snow cover are potentially a significant factor affecting the decoupling between SAT and cave temperature.

7. Conclusions

The connexion between SAT and cave temperature was investigated at Eagle Cave (Spain). The temperature of this cave depends mostly on conduction of surface ground temperature through the bedrock. Based on the thermal amplitude of the seasonality of three galleries sited at different depths, together with sub-surface and surface records, the thermal coefficient diffusion of Eagle Cave was calculated. The temperature recorded in the surface has a delay before reaching the cave galleries. This lag time is in the order of 3–11 yr for galleries with ~5–18 m of bedrock cover over the ceiling. The cave temperature signal from galleries at different depths monitored during the last 3 yr record changes in SAT at various periods, showing the connexion and response of cave temperature to SAT changes.

The cave temperature depends on the surface ground temperature. The SAT influences Eagle Cave temperature but other factors affect the ground surface temperature. A difference > 3 °C was found between forested and grassland sites at depths of 0.5 m. Therefore, the net solar radiation received at ground surface and its heat transfer within the soil can vary significantly depending on the changes in vegetation cover. The evolution of forest cover over Eagle Cave together with the mean annual SAT in Tietar Valley during the past decades allow the reconstruction of 45 yr of cave temperature based on thermal conduction from ground surface temperatures. The thermal reconstruction reproduces a ~2 °C cooling of the cave since late-1960s. The changes in SAT contributed to this thermal shift although most of the cooling is thought to be the result of the afforestation of the cave hill. This temperature reconstruction is in agreement with the existing monitoring data.

Most of the change in cave temperature during the past decades is the result of a variable decoupling of SAT and surface ground temperature, caused by the change in vegetation cover, which is climate independent. This has a significant impact on speleothem proxies that are temperature-dependent. Theoretically, a speleothem from Eagle Cave precipitated during the past 45 yr would record an $\delta^{18}\text{O}$ increase of 0.36‰, if equilibrium conditions are considered, as a result of the cave temperature changes exclusively due to afforestation. Such a change in the speleothem isotope composition would be almost doubled if the vegetation change would have been from grassland to forest. This example highlights the importance of a variable cave temperature decoupling in interpreting speleothem records. Thermal decoupling is expected in sites with changes in vegetation cover over cave. Therefore, changes in land use, fires or ecotone shifts due to natural changes are potentially recorded in temperature dependent proxies of speleothems. A variable decoupling between SAT and cave temperature can also result from a significant modification on the duration of the snow cover over the cave. Both circumstances are of major importance during glacial-interglacial transitions, where vegetation changes and modification of the snow covers duration are significant. Thus, further discussion on the possible effects of variable thermal decoupling should be considered when interpreting temperature dependent proxies in speleothems. We recommend a detailed description of the thermal dynamic of the cave and a discussion of possible effects of a variable decoupling between SAT and cave temperature when precise

palaeoclimate reconstructions are based on thermal dependent proxies from speleothems.

Acknowledgements

The research leading to these results has received funding from the European Community under a Marie Curie Intra-European Fellowship of the Seventh Framework Programme FP7/2007–2013 (Grant agreement no. 219891; PROCAVET project). Additional funds were provided from project CGL2008-03396/BTE (GLACIO-SICE) funded by MICINN and PII109-0138-6113 (CRONOGREDOS) funded by JCCM. We would like to thank the cave managers whose collaboration facilitated the execution of this study. Meteorological data from Tietar Valley was provided by the Agencia Estatal de Meteorología (AEMET).

Appendix A. Supplementary material

Supplementary data associated with this article can be found in the online version at <http://dx.doi.org/10.1016/j.epsl.2013.03.017>.

References

- Anderson, M.P., 2005. Heat as a ground water tracer. *Ground Water* 43, 951–968.
- Atkinson, T.C., Smart, P.L., Wigley, T.M.L., 1983. Climate and natural radon levels in Casteguard Cave, Columbia icefields, Alberta, Canada. *Artic Alp. Res.* 15, 487–502.
- Badino, G., 1995. *Fisica del Clima Sotterraneo*. vol. 7 Serie II. Memoria dell'Istituto Italiano di Speleologia, Bologna.
- Badino, G., 2005. Underground drainage systems and geothermal flux. *Acta Carsologica* 34, 277–316.
- Baker, A., Genty, D., Dreybrodt, W., Barnes, W.L., Mockler, N.J., Grapes, J., 1998. Testing theoretically predicted stalagmite growth rate with recent annually laminated samples: implications for past stalagmite deposition. *Geochim. Cosmochim. Acta* 62, 393–404.
- Baker, A., Asrat, A., Fairchild, I.J., Leng, M.J., Wynn, P.M., Bryant, C., Genty, D., Umer, M., 2007. Analysis of the climate signal contained within delta O-18 and growth rate parameters in two Ethiopian stalagmites. *Geochim. Cosmochim. Acta* 71, 2975–2988.
- Baker, A., Bradley, C., 2010. Modern stalagmite $\delta^{18}\text{O}$: instrumental calibration and forward modelling. *Global Planet. Change* 71, 201–206.
- Baldini, J.U.L., McDermott, F., Baker, A., Baldini, L.M., Matthey, D.P., Railsback, L.B., 2005. Biomass effects on stalagmite growth and isotope ratios: a 20th century analogue from Wiltshire, England. *Earth Planet. Sci. Lett.* 240, 486–494.
- Beltrami, H., 2001. Surface heat flux histories from inversion of geothermal data: energy balance at the Earth's surface. *J. Geophys. Res.* 106 (B10), 21979–21993.
- Beltrami, H., Kellman, L., 2003. An examination of short- and long-term air-ground temperature coupling. *Global Planet. Change* 38, 291–303.
- Boch, R., Spötl, C., Frisia, S., 2011. Origin and palaeoenvironmental significance of lamination in stalagmites from Katerloch Cave, Austria. *Sedimentology* 58, 508–5031.
- Bögli, A., 1980. *Karst Hydrology and Physical Speleology*. Springer Verlag, Berlin.
- Bourges, F., Genthon, P., Mangin, A., D'Hulst, D., 2006. Microclimates of L'Aven D'Orgnac and other French limestone caves (Chaveaut, Esparrros, Marsoulas). *Int. J. Climatol.* 26, 1651–1670.
- Brunet, M., Jones, P.D., Sigró, J., Saladié, O., Aguilar, E., Moberg, A., Della-Marta, P.M., Lister, D., Walthers, A., López, D., 2007. Temporal and spatial temperature variability and climate change over Spain during 1850–2005. *J. Geophys. Res.* 112, D12117.
- Buecher, R.H., 1999. Microclimate study of Kartchner Caverns, Arizona. *J. Cave Karst Stud.* 6, 108–120.
- Cai, B., Pumijumong, N., Tan, M., Muangsong, C., King, X., Jiang, X., Nan, S., 2010. Effects of intraseasonal variation of summer monsoon rainfall on stable isotope and growth rate of a stalagmite from northwestern Thailand. *J. Geophys. Res.* 115, D21104.
- Carlslaw, H.S., Jaeger, J.C., 1959. *Conduction of Heat in Solids*, second ed. Oxford University Press, New York.
- Cermak, V., Rybach, L., 1982. Thermal conductivity and specific heat of minerals and rocks. In: Angenheister, G. (Ed.), *Landolt-Börnstein: Zahlenwerte und Funktionen aus Naturwissenschaften und Technik*. Springer-Verlag, Berlin, pp. 305–343.
- Cigna, A., 1961. Air temperature distributions near entrance of caves. In: *Proceedings of the Symposium International of Speleology*, vol. 5 (2). Varenna 1960, *Memories of the Rassegna Speleologica Italiana*, pp. 259–267.
- Cigna, A., 1993. Environmental management of tourist caves. The examples of Grotta di Castellana and Grotta del Vento, Italy. *Environ. Geol.* 21, 173–180.

- Cropley, J.B., 1965. Influence of surface conditions on temperatures in large cave systems. *Bull. Natl. Speleol. Soc.* 27, 1–10.
- De Freitas, C.R., Littlejohn, R.N., 1987. Cave climate: assessment of heat and moisture exchange. *J. Climatol.* 7, 553–569.
- De Freitas, C.R., Schmokal, A., 2003. Condensation as a microclimate process: measurement, numerical simulation and prediction in the Glowworm Cave, New Zealand. *Int. J. Climatol.* 23, 557–575.
- Denniston, R.F., González, L.A., Baker, R.G., Asmerom, Y., Reagan, M.K., Edwards, R.L., Alexander, E.C., 1999. Speleothem evidence for Holocene fluctuation of the prairie-forest ecotone, north-central USA. *Holocene* 9, 671–676.
- Domínguez-Villar, D., 2012. Heat flux. In: Fairchild, I.J., Baker, A. (Eds.), *Speleothem Science: From Process to Past Environments*. Wiley-Blackwell, Chichester, pp. 137–145.
- Domínguez-Villar, D., Fairchild, I.J., Carrasco, R.M., Pedraza, J., Baker, I., 2010. The effect of visitors in a tourist cave and the resulting constraints on natural thermal conditions for palaeoclimate studies (Eagle Cave, central Spain). *Acta Carsologica* 39, 491–502.
- Dorale, J.A., González, L.A., Reagan, M.K., Pickett, D.A., Murrell, M.T., Baker, R.G., 1992. A high-resolution record of Holocene climate change in speleothem calcite from Cold Water Cave, north-east Iowa. *Science* 258, 1626–1630.
- Dreybrodt, W., 1981. The kinetics of calcite precipitation from thin films of calcareous solution and the growth of speleothems: revisited. *Chem. Geol.* 32, 237–245.
- Epstein, S., Buchsbaum, R., Lowenstam, H., Urey, H.C., 1953. Revised carbonate-water isotopic temperature scale. *Bull. Geol. Soc. Am.* 64, 1315–1326.
- Eraso, A., 1962. Ideas sobre la climática subterránea. *Estudios del grupo Espeleológico, Alavés* 21–41.
- Fairchild, I.J., Frisia, S., Borsato, A., Tooth, A.F., 2007. Speleothems. In: Nash, D.J., McLaren, S.J. (Eds.), *Geochemical Sediments and Landscapes*. Blackwell, Oxford, pp. 200–245.
- Fairchild, I.J., Treble, P.C., 2009. Trace elements in speleothems as recorders of environmental change. *Q. Sci. Rev.* 28, 449–468.
- Fairchild, I.J., Baker, A., 2012. *Speleothem Science: From Processes to Past Environments*. Wiley-Blackwell, Chichester.
- Ferguson, G., Beltrami, H., 2006. Transient lateral heat flow due to land-use changes. *Earth Planet. Sci. Lett.* 242, 217–222.
- Frisia, S., Borsato, A., Preto, N., McDermott, F., 2003. Late Holocene annual growth in three Alpine stalagmites records the influence of solar activity and the North Atlantic Oscillation on winter climate. *Earth Planet. Sci. Lett.* 216, 411–424.
- Genty, D., 2008. Paleoclimate research in Villars Cave (Dordogne, SW-France). *Int. J. Speleol.* 37, 173–191.
- Huang, Y., Fairchild, I.J., 2001. Partitioning of Sr^{2+} and Mg^{2+} into calcite in karst-analogue experiment solutions. *Geochim. Cosmochim. Acta* 65, 47–62.
- Jex, C.N., Baker, A., Fairchild, I.J., Eastwood, W.J., Leng, M.J., Sloane, H.J., Thomas, L., Bekaroglu, E., 2010. Calibration of speleothem $\delta^{18}\text{O}$ with instrumental climate records from Turkey. *Global Planet. Change* 71, 207–217.
- Jex, C.N., Baker, A., Eden, J.M., Eastwood, W.J., Fairchild, I.J., Leng, M.J., Thomas, L., Sloane, H.J., 2011. A 500 yr speleothem-derived reconstruction of a late autumn-winter precipitation, North East Turkey. *Q. Res.* 75, 399–405.
- Kaufmann, G., 2003. Stalagmite growth and palaeo-climate: the numerical perspective. *Earth Planet. Sci. Lett.* 214, 251–266.
- Kim, S.T., O'Neil, J.R., 1997. Equilibrium and nonequilibrium oxygen isotope effects in synthetic carbonates. *Geochim. Cosmochim. Acta* 61, 3461–3475.
- Kranjc, A., Opara, B., 2002. Temperature monitoring in Škocjanske Jame caves. *Acta Carsologica* 31, 85–96.
- Labs, K., 1982. Regional-analysis of ground and above-ground climate. *Underground Space* 7, 37–65.
- Lauritzen, S.E., Lundberg, J., 1999. Calibration of the speleothem delta function: an absolute temperature record for the Holocene in northern Norway. *Holocene* 9, 659–669.
- Lewis, T.J., Wang, K., 1998. Geothermal evidence for deforestation induced warming: Implications for the climatic impact of land development. *Geophys. Res. Lett.* 25, 535–538.
- Luetscher, M., Jeannin, P.Y., 2004. Temperature distribution in karst systems: the role of air and water fluxes. *Terra Nova* 16, 344–350.
- Luetscher, M., Lismonde, B., Jeannin, P.Y., 2008. Heat exchanges in the heterothermic zone of a karst system: Monlesi cave, Swiss Jura Mountains. *J. Geophys. Res.* 113, F02025.
- Mangini, A., Spötl, C., Verde, P., 2005. Reconstruction of temperature in the Central Alps during the past 2000 years from a $\delta^{18}\text{O}$ stalagmite record. *Earth Planet. Sci. Lett.* 235, 741–751.
- Martín Escorza, C., 1971. Estudio mesotectónico en los materiales metamórficos de los alrededores de Arenas de San Pedro (Prov. De Ávila-Toledo). *Bol. Real Soc. Esp. Hist. Nat. (Secc. Geol.)* 69, 303–327.
- Mattey, D., Lowry, D., Duffet, J., Fisher, R., Hodge, E., Frisia, S., 2008. A 53 year seasonally resolved oxygen and carbon isotope record from a modern Gibraltar speleothem: reconstructed drip water and relationship to local precipitation. *Earth Planet. Sci. Lett.* 269, 80–95.
- Mazarrón, F., Cañas, I., 2009. Seasonal analysis of the thermal behaviour of traditional underground wine cellars in Spain. *Renewable Energy* 34, 2484–2492.
- McDermott, F., Atkinson, T.C., Fairchild, I.J., Baldini, L.M., Mattey, D.P., 2011. A first evaluation of the spatial gradients in $\delta^{18}\text{O}$ recorded by European Holocene speleothems. *Global Planet. Change* 79, 275–287.
- Myers, J.O., 1962. Cave physics. In: Cullinford, C.H.D. (Ed.), *British Caving. An Introduction to Speleology*. Routledge and Kegan Paul, London, pp. 226–250.
- Moore, G.W., 1964. Cave temperature. *Natl. Speleol. Soc. News* 22, 57–60.
- Moore, G.W., Nicholas, G., 1964. Out of phase seasonal temperature fluctuations in Cathedral Cave, Kentucky. *Geol. Soc. Am. Spec. Pap.* 76, 313.
- Moore, G.W., Sullivan, G.N., 1978. *Speleology: the Study of Caves*. Zephyrus Press, Teaneck, NJ (USA).
- Munroe, J.S., 2012. Physical, chemical, and thermal properties of soils across a forest-meadow ecotone in the Uinta Mountains, Northeastern Utah, USA. *Artic. Antarct. Alp. Res.* 44, 95–106.
- Nitoui, D., Beltrami, H., 2005. Subsurface thermal effects of land use changes. *J. Geophys. Res.* 110, F01005.
- Odrizola, J.M., Peón, A., Ugidos, J.M., Pedraza, J., Fernández, P., 1980. Arenas de San Pedro 578, 1:50000. MAGNA, Madrid.
- Oster, J.L., Montañez, I.P., Guilderson, T.P., Sharp, W.D., Banner, J.L., 2010. Modeling speleothem $\delta^{13}\text{C}$ variability in a central Sierra Nevada cave using ^{14}C and $^{87}\text{Sr}^{86}\text{Sr}$. *Geochim. Cosmochim. Acta* 74, 5228–5242.
- Perrier, F., Morat, P., Mouél, J.L., 2001. Pressure induced temperature variation in an underground quarry. *Earth Planet. Sci. Lett.* 191, 145–156.
- Perrier, F., Le Mouél, J.L., Poirier, J.P., Shnirman, M.G., 2005. *Int. J. Climatol.* 25, 1619–1631.
- Pflitsch, A., Piasecki, J., 2003. Detection of an airflow system in Niedzwiedzia (Bear) Cave, Kletno, Poland. *J. Cave Karst Stud.* 65, 160–173.
- Pollack, H.N., Huang, S., 2000. Climate reconstruction from subsurface temperatures. *Annu. Rev. Earth Planet. Sci.* 28, 339–365.
- Pollack, H.N., Smerdon, J.E., van Keken, P.E., 2005. Variable seasonal coupling between air and ground temperatures: a simple representation in terms of subsurface thermal diffusivity. *Geophys. Res. Lett.* 32, L15405.
- Salve, R., Krakauer, N.Y., Kowalsky, M.B., Finsterle, S., 2008. A quantitative assessment of microclimatic perturbation in a tunnel. *Int. J. Climatol.* 28, 2081–2087.
- Sánchez-Moral, S., Soler, V., Cañaveras, J.C., Sanz-Rubio, E., van Grieten, R., Gysels, K., 1999. Inorganic deterioration affecting the Altamira Cave, N. Spain: quantitative approach to wall-corrosion (solutional etching) processes induced by visitors. *Sci. Total Environ.* 244, 67–84.
- Schouten, S., Hugué, C., Hopmans, E., Kienhuis, M.V.M., Sinninghe Damsté, J.S., 2007. Analytical methodology for TEX(86) paleothermometry by high-performance liquid chromatography/atmospheric pressure chemical ionization-mass spectrometry. *Anal. Chem.* 79, 2940–2944.
- Smerdon, J.E., Pollack, H.N., Enz, J.W., Lewis, M.J., 2003. Conduction-dominated heat transport of the annual temperature signal in soil. *J. Geophys. Res.* 108 (B9), 2431.
- Smerdon, J.E., Pollack, H.N., Cermak, V., Enz, J.W., Kresl, M., Safanda, J., Wehmler, J.F., 2004. Air-ground temperature coupling and subsurface propagation of annual temperature signals. *J. Geophys. Res.* 109, D21107.
- Smerdon, J.E., Stieglitz, M., 2006. Simulating heat transport of harmonic temperature signals in the Earth's shallow subsurface: lower-boundary sensitivities. *Geophys. Res. Lett.* 33, L14402.
- Smerdon, J.E., Pollack, H.N., Cermak, V., Enz, J.W., Krel, M., Safanda, J., Wehmler, J.F., 2006. Daily, seasonal, and annual relationships between air and subsurface temperatures. *J. Geophys. Res.* 111, D07101.
- Smithson, P.A., 1991. Inter-relationships between cave and outside air temperatures. *Theor. Appl. Climatol.* 44, 65–73.
- Spötl, C., Fairchild, I.J., Tooth, A., 2005. Cave air on drip water geochemistry, Obir caves (Australia): implications for speleothem deposition in dynamically ventilated caves. *Geochim. Cosmochim. Acta* 69, 2451–2468.
- Stevens, M.B., González-Rouco, J.F., Beltrami, H., 2008. North America climate of the last Millennium: underground temperatures and model comparison. *J. Geophys. Res.* 113, F01008.
- Treble, P., Shelley, J.M.G., Chappell, J., 2003. Comparison of high resolution sub-annual records of trace elements in a modern (1911–1992) speleothem with instrumental climate data from southwest Australia. *Earth Planet. Sci. Lett.* 216, 141–153.
- Vieira, G.T., Mora, C., Ramos, M., 2003. Ground temperature regimes and geomorphological implication in a Mediterranean mountain (Serra da Estrela, Portugal). *Geomorphology* 52, 57–72.
- Villaverde, J., Crespo, J., Navares, A., Gracia, A., 2009. Topografía de la Cueva del Águila. Technical Report, unpublished.
- Wigley, T.M.L., Brown, M.C., 1971. Geophysical applications of heat and mass transfer in turbulent pipe flow. *Boundary-Layer Meteorol.* 1, 300–320.
- Wigley, T.M.L., Brown, M.C., 1976. The physics of caves. In: Ford, T.D., Cullinford, C.H.D. (Eds.), *The Science of Speleology*. Academic Press, London, pp. 329–358.